4.8

ARCTIC STORM SIMULATION WITH THE ARCTIC MM5 MODEL: PERFORMANCE VALIDATION

Jing Zhang [1], Jeffrey S. Tilley [1] and Xiangdong Zhang [2]

1 Geophysical Institute, University of Alaska Fairbanks, Fairbanks, AK 99775
2 International Arctic Research Center, University of Alaska Fairbanks, Fairbanks, AK 99775

1. Introduction

Various observational and modeling studies have noted several prominent changes in the Arctic climate system over the past few decades. A decline of sea ice volume (e.g., Rothrock et al, 1999) has been hypothesized to be related to an amplified global warming in the Northern Hemisphere (e.g., Manabe and Stouffer, 1994). Also, average sea level pressure has dropped over the central Arctic during the past few decades (Walsh et al., 1996). Concurrent with the decreasing sea ice extent, and changing air circulation patterns, there have been positive trends in the frequency and cyclonic storms in high latitudes (e.g., Serreze and Barry, 1988). McCabe et al., 2001 also suggest that the increase in high latitude cyclone frequency, associated with a northward shift of storm tracks, is a regional trend for the Arctic under conditions of global warming. This implies that interactions between Arctic storms and the large-scale circulation may play an important role in the evolution of a global warming scenario in high latitudes.

As such, studies of the development processes within Arctic storms, as well as their interaction with the background atmospheric circulation, land surface, sea ice and ocean, are needed. In our work we plan to investigate these questions with a coupled modeling system denoted the "Arctic MM5". The Arctic MM5 includes land surface, thermodynamic sea ice and ocean mixed layer components coupled to the atmosphere. In this paper, we briefly describe aspects of the model and evaluate the Arctic MM5 performance on the simulation of two Pacifc/Arctic cyclonic storm systems.

In the following section we first describe aspects of the Arctic MM5 system. The simulations of the Arctic storms used as case studies will be given in section 3, with a brief discussion in section 4.

2. The Arctic MM5 Model

2.1. General Comments

As noted above, the Arctic MM5 model includes an atmospheric model, the PSU/NCAR MM5 (e.g., Grell et al 1994) that has been coupled to land surface, sea ice and ocean mixed-layer models: (1) a version of the land surface model NOAH (e.g., Mitchell et al., 2002), (2) a thermodynamic sea ice model (Zhang and Zhang, 2001) and (3) an ocean mixed layer model (Kantha and Clayson, 1994).

The NOAH land surface model includes cold season processes such as the spatial and temporal variability of the snowpack as well as frozen soils. A detailed description of the NOAH model NOAH-LSM, and its coupling to the PSU/NCAR MM5, have been given of Chen and Dudhia (2001), Mitchell et al. (2002) and Koren et al. (1999). We refer the reader to these papers for details on the NOAH scheme.

2.2. Sea Ice and Mixed Layer Models

The thermodynamic sea ice model (Zhang and Zhang, 2001) predicts changes in sea ice concentration and sea ice temperature. As briefly noted in Zhang et al (2001) and Zhang and Tilley (2002), the treatment of sea ice thermodynamics is similar to that in both Hibler (1979) and Parkinson and Washington (1979). Sea ice thickness *h* and concentration *A* at a grid cell are described by the following equations:

$$\frac{\partial h}{\partial t} = F_h \qquad (1)$$

$$\frac{\partial A}{\partial t} = F_A \qquad (2)$$

F_h and F_A are the thermodynamic source/sink functions, parameterized following Hibler (1979):

$$F_A = \frac{F_h}{2h} A + \frac{\left(\partial h / \partial t\right)_{therm}^{0}}{h_0}(1-A) \qquad (3)$$

$$F_h = \left(\frac{\partial h}{\partial t}\right)_{therm}^{1} A + \left(\frac{\partial h}{\partial t}\right)_{therm}^{0} (1-A) \qquad (4)$$

where h_0 = thickness of new sea ice (= $0.2m$). Superscript "0" represents new ice forming over open water while superscript "1" represents growth of existing sea ice. $\left(\frac{\partial h}{\partial t}\right)_{therm}$, the local rate of sea ice growth or melt, is determined from an energy balance calculation:

$$\left(\frac{\partial h}{\partial t}\right)_{therm} = \frac{1}{q_0}(H_w - H_n) \qquad (5)$$

where q_0 is the latent heat of fusion for ice (Values for constants are provided in Appendix A).

H_n has different definitions depending on the surface types:

$H_n = H_{To}$ = *net surface energy flux, open ocean*
$H_n = H_{Ti}$ = *net surface energy flux, bare sea ice*
$H_n = G_i$ = *conductive heat flux within snow-covered sea ice*

Details on H_{To}, H_{Ti} and G_i are given in Appendix B.

H_w is the turbulent heat flux between the sea ice bottom surface and the ocean, formulated following Ebert and Curry (1993):

$$H_w = \rho_o c_{po} C_t (T_f - T_o) \qquad (6)$$

where ρ_o is the ocean water density, c_{po} the ocean specific heat, C_t a bulk transfer coefficient and T_f the freezing temperature. T_o is the ocean temperature which is calculated by the ocean mixed layer model.

The snow surface temperature T_s and the sea ice surface temperature T_i need to be defined to close the equation set. A Newton/Raphson iterative scheme is used to obtain T_s and T_i from surface energy balance. When there is no snow cover on the sea ice, T_i is calculated by linearizing the sea ice surface energy balance as:

$$T_i^n = T_i^{n-1} + \frac{H_{Ti}{}^{n-1} + \frac{C_i}{h}(T_b - T_i^{n-1})}{4\sigma(T_i^{n-1})^3 + \frac{C_i}{h} + \rho C_p C_h V + \rho C_p L_s q_i \frac{a(273.16-b)}{(T_i^{n-1}-b)^2}} \qquad (7)$$

where T_i^n, T_i^{n-1} are the sea ice surface temperatures at the current iteration step and previous step, respectively. $H_{Ti}{}^{n-1}$ is the sea ice surface net energy flux calculated with T_i^{n-1}. a and b are constants used in the specific humidity computation.

When the sea ice is snow-covered, a similar relation is used to obtain T_s:

$$T_s^n = T_s^{n-1} + \frac{H_{Ts}{}^{n-1} + \frac{C_s C_i}{C_i h_s + C_s h}(T_b - T_s^{n-1})}{4\sigma(T_s^{n-1})^3 + \frac{C_s C_i}{C_i h_s + C_s h} + \rho C_p C_h V + \rho C_p L_s q_s \frac{a(273.16-b)}{(T_s^{n-1}-b)^2}} \qquad (8)$$

where T_s^n, T_s^{n-1} and $H_{Ts}{}^{n-1}$ are defined analogously to their counterparts in (7).

The interface between snow and sea ice has a balance between the conductive fluxes of snow and sea ice:

$$\frac{C_s}{h_s}(T_i - T_s) = \frac{C_i}{h}(T_b - T_i) \qquad (9)$$

Using (7) and (8), we have:

$$T_i^n = \frac{C_s h T_s^n + C_i h_s T_b}{C_s h + C_i h_s} \qquad (10)$$

Thus from (1)-(10), the changes of sea ice thickness and concentration, sea ice/snow temperatures and flux exchanges between the atmosphere and the surface can be predicted.

The ocean mixed layer model predicts the change of ocean temperature T_o, salinity, density, mixed layer depth as well as heat flux exchanges between the ocean and the sea ice. T_o is used in the calculations of H_{To} and H_w in the sea ice model. The mixed layer model (hereafter denoted *MLM*) employed in the Arctic MM5 is the second-moment closure model developed by Kantha and Clayson (1994). This MLM model is based on Mellor-Yamada's second-order turbulence closure with improved parameterizations of pressure covariance terms and the inclusion of shear instability-induced mixing in the strongly stratified

region below the ocean mixed layer. The governing equations of the MLM model include conservation laws for mass, momentum, and scalar mean quantities as well as conservation relations for second-order turbulence quantities, Reynolds stress, turbulent heat fluxes and the temperature variance. We refer the reader to the Kantha and Clayson (1994) paper for details.

3. Storm simulations

The Pacific/Arctic storm cases of December 16-21 1999 and February 8-13 2001 have been chosen as our simulation objects. In this article, we only include preliminary simulation results from the storm case of December 16-21 1999. Further analysis results and the second case simulations will be presented at the conference.

The simulation domain covers the Arctic Ocean, Alaska, northwest Canada, north Pacific Ocean and east Russia, as shown in Figure 1. We utilize a model grid resolution of 35km for this domain on a computational grid of 165(X) x 165(Y) x 31(Z). A model time step of 100s is used.

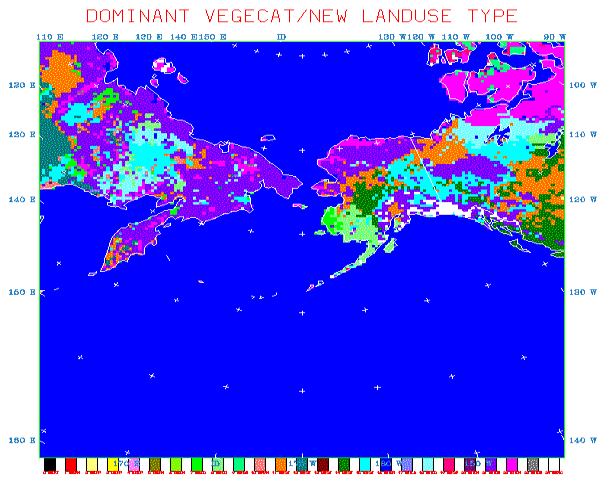

Figure 1. Simulation Domain for the Arctic MM5 Simulations. Colors indicate land use types.

In all simulations, we employed the following physical parameterizations: the Dudhia (1989) simple ice microphysics scheme; the Grell (1993) cumulus scheme; the MRF planetary boundary layer scheme (Hong and Pan 1996); a simple cloud radiative cooling scheme (Benjamin 1983); and the land surface model NOAH-LSM (Mitchell et al., 2002, Koren et al., 1999), in which a thermodynamic sea ice model and mixed layer ocean model as described in section 2 are coupled. NCEP/NCAR reanalysis data are used to provide initial and boundary conditions to the modeling system. Initial sea ice concentration is from NCEP/NCAR climate data assimilation system (CDAS) in which sea ice concentration grids are constructed from the SSMI sensor on the DMSP F-13 (11) satellite.

By analyzing sea level pressure from the NCEP/NCAR reanalysis, we can obtain the storm trajectory. For the case of Dec.16-21 1999, the storm trajectory is shown in Figure 2. It is shown the storm is originated in the western Pacific Ocean at 00UTC Dec.16 and then moves westward to the 180W longitude line at 00UTC Dec.17. Then this storm system begins to move northward and lands on the southwest Alaska at 12UTC Dec.19. From 12UTC Dec.19- 18UTC Dec.20 the storm affected the whole east coast of Alaska and finally ends in the Arctic Ocean at 18UTC Dec. 21.

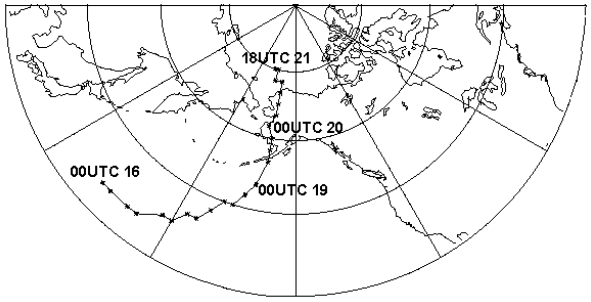

Figure 2. Analyzed storm trajectory for case of December 16-21 1999

We perform simulations for this storm event from 00UTC December 19-00UTC December 22 1999 with the Arctic MM5 model. And the results show that the model basically simulates the whole processes of the storm movement. As shown in Figure 3a, a low center of sea level pressure (SLP) (973 mb) is just located at the south of Aleutian Islands at the beginning of simulation and then this SLP low lands on the mainland of Alaska, continuously moves northward and covers the Norton Sound coast areas (with the low center 975 mb) at 00UTC December 20 (Figure 3b), which matches the analysis data as shown in Figure 2 very well. Northward movement continues and the SLP low center (985 mb) moves into the Arctic Ocean at 00UTC December 21 (Figure 3c), which is also consistent with the analysis as shown in Figure 2. At 00UTC December 22, as in Figure 3d, the SLP low center is still located in the Arctic Ocean but the strength of the low center decreased to 995 mb. The Arctic MM5 model has simulated the storm motion (track) reasonably.

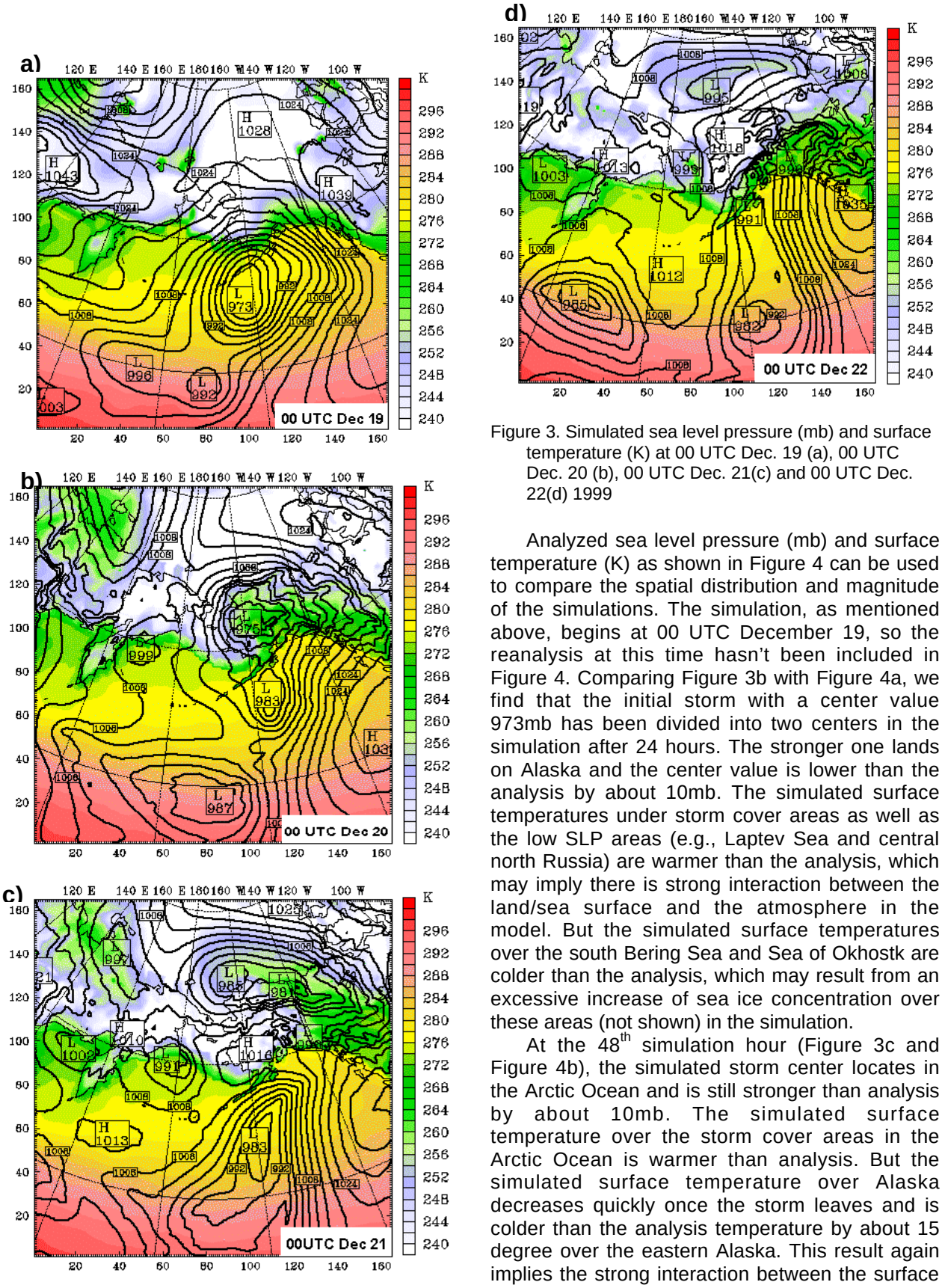

Figure 3. Simulated sea level pressure (mb) and surface temperature (K) at 00 UTC Dec. 19 (a), 00 UTC Dec. 20 (b), 00 UTC Dec. 21(c) and 00 UTC Dec. 22(d) 1999

Analyzed sea level pressure (mb) and surface temperature (K) as shown in Figure 4 can be used to compare the spatial distribution and magnitude of the simulations. The simulation, as mentioned above, begins at 00 UTC December 19, so the reanalysis at this time hasn't been included in Figure 4. Comparing Figure 3b with Figure 4a, we find that the initial storm with a center value 973mb has been divided into two centers in the simulation after 24 hours. The stronger one lands on Alaska and the center value is lower than the analysis by about 10mb. The simulated surface temperatures under storm cover areas as well as the low SLP areas (e.g., Laptev Sea and central north Russia) are warmer than the analysis, which may imply there is strong interaction between the land/sea surface and the atmosphere in the model. But the simulated surface temperatures over the south Bering Sea and Sea of Okhostk are colder than the analysis, which may result from an excessive increase of sea ice concentration over these areas (not shown) in the simulation.

At the 48th simulation hour (Figure 3c and Figure 4b), the simulated storm center locates in the Arctic Ocean and is still stronger than analysis by about 10mb. The simulated surface temperature over the storm cover areas in the Arctic Ocean is warmer than analysis. But the simulated surface temperature over Alaska decreases quickly once the storm leaves and is colder than the analysis temperature by about 15 degree over the eastern Alaska. This result again implies the strong interaction between the surface

and atmosphere in the model. Meanwhile we also notice a low center over the southwest Bering Sea and it is related to the upper atmosphere structure by analyzing the geopotential height in the upper atmosphere.

At the end of this simulation, the simulated storm center over the Arctic Ocean is decaying (Figure 3d), but still a bit stronger than analysis (Figure 4c) by about 5mb. The high SLP in the simulation dominates the most part of Alaska with very low surface temperature, not like in the analysis, in which only northwest Alaska is exposed to the high SLP and cold temperature.

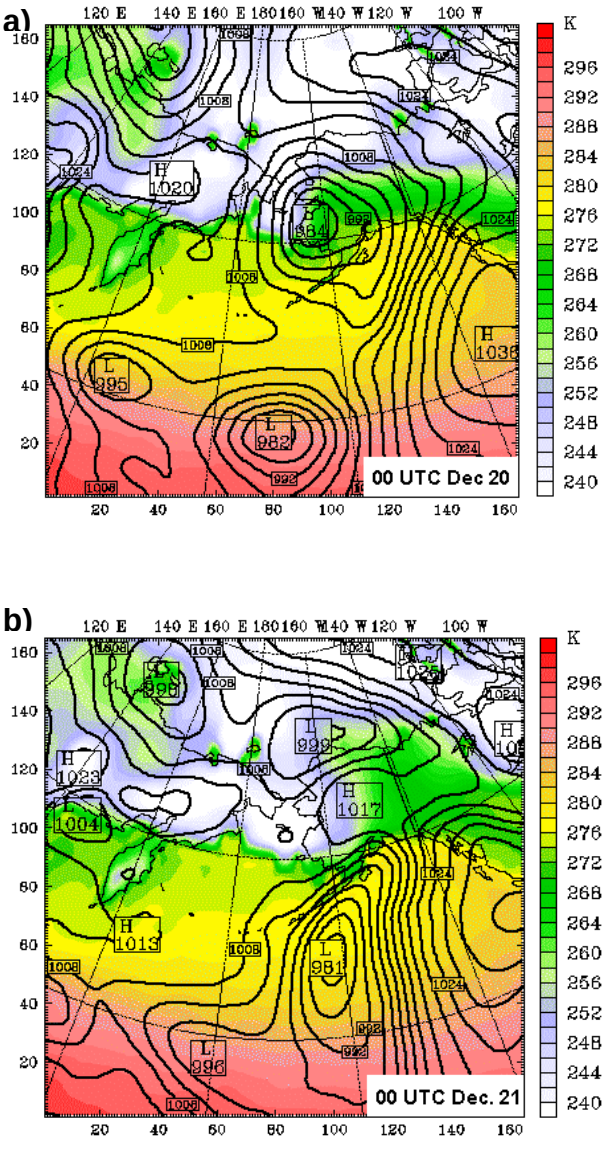

Figure 4. Analysis sea level pressure (mb) and surface temperature (K) at a) 00 UTC Dec. 20, b)00 UTC Dec. 21 and c) 00 UTC Dec. 22 1999

References:

Benjamin, S. G., 1983: Some effects of surface heating and topography on the regional severe storm environment. Ph.D. Thesis, Department of Meteorology, The Pennsylvania State University, 265 pp.

Chen, F. and J. Dudhia, 2001: coupling an advanced land-surface hydrology model with the PSU/NCAR MM5 modeling system. Part I: Model description and imple-mentation, *Mon. Wea. Rev.,* **129,** 569-585.

Dudhia, J., 1989: Numerical study of convection observed during the winter monsoon experiment using a mesoscale two-dimensional model. *J. Atmos. Sci.,* **46**, 3077-3107.

Ebert, E. E., and J. A. Curry, 1993: An intermediate one-dimensional thermodynamic sea ice model for investigating ice-atmosphere interactions, *J. Geophys. Res.,* **98**, 10,085-10,109.

Grell, G., 1993: Prognostic evaluation of assumptions used by cumulus parameterizations. *Mon. Wea. Rev.,* **121**, 764-787.

Hibler, W. D. III, 1979: A dynamic thermodynamic sea ice model, *J. Phys. Oceanogr.,* **9**, 815-846.

Hong, S.Y., and H.-L.Pan, 1996: Nonlocal boundary layer vertical diffusion in a medium-range forecast model, *Mon. Wea. Rev.,* **124**, 2322-2339.

Kantha, L., and C. Clayson, 1994: An improved mixed layer model for geophysical applications, *J. Geophys. Res.*, **99**, 25235-25266.

Koren, V., J. Schaake, K. Mitchell, Q.-Y. Duan, F. Chen, and J. M. Baker, 1999: A parameterization of snowpack and frozen ground intended for NCEP weather and climate models, *J. Geophys. Res.*, **104,** 19,569-19,585.

Manabe, S., and R. Stouffer, 1994: Multiple century response of a coupled ocean-atmosphere model to an increase of atmospheric carbon dioxide, *J. Clim.,* **7**, 5-23.

McCabe, Gregory J., Martyn P. Clark, Mark C. Serreze, 2001: Trends in Northern Hemisphere Surface Cyclone Frequency and Intensity. *Journal of Climate*, **14,** 2763–2768.

Mitchell, K., et al, Reducing near-surface cool/moist biases over snowpack and early spring wet soils in NCEP ETA model forecasts via land surface model upgrades, *16th conference on hydrology*, Orlando, 2002.

Parkinson, C. L., and W. M. Washington, 1979: A large scale numerical model of sea ice, *J. Geophys. Res.,* **84,** 311-337.

Rothrock, D.A., Y. Yu, G.A. Maykut, 1999. Thinning of the arctic sea-ice cover, *Geophys. Res. Lett.*, **26**(23), 3469-72**.**

Serreze, Mark C., and Roger G. Barry, 1988: Synoptic Activity in the Arctic Basin, 1979–85. *Journal of Climate*, **1**, 1276–1295.

Walsh, John E., William L. Chapman, Timothy L. Shy, 1996: Recent Decrease of Sea Level Pressure in the Central Arctic. *Journal of Climate*, **9**, 480–488.

Zhang, J., J. S. Tilley and X. Zhang, 2001: Towards improvement of sea-ice physics in MM5 for the Arctic regional modeling. *Preprints*, *11th PSU/NCAR Mesoscale Model Users' Workshop,* AMS, 25-27 June, Boulder, CO, 122-125.

Zhang, J. and J. S. Tilley, 2002: *Arctic MM5 Modeling System: Part 3: Coupling of a Thermodynamic Sea Ice Model with the Mesoscale Model MM5.* Technical Report to University Partnering for Operational Support Program, Johns Hopkins University, September 2002, 117 pp

Zhang, X., and J. Zhang, 2001: Heat and freshwater budgets and pathways in the Arctic Mediterranean in a coupled ocean/sea-ice model, *J. Oceanography,* **57**, 207-237.

Acknowledgments:

The work was sponsored by grants from both IARC and Johns Hopkins University under the University Partnering for Operational Support Initiative. Thanks go to Drs. Kantha and Clayson for the ocean mixed layer model MLM.

Appendix A: Sea Ice/MLM Constants

Here we provide a list of values of significant constants used within the sea ice and MLM models.

q_0 = *heat of fusion for ice* = $302\times10^6 m^3 J^{-1}$,

ρ_o = *ocean water density* = $1026.0 kgm^{-3}$

c_{po} = *ocean specific heat* = $4218.0 Jkg^{-1}K^{-1}$

C_t = *bulk transfer coefficient* = $1.16\times10^{-5} ms^{-1}$,

$a = 21.87$; $b = 7.66$= *specific humidity constants*.

α_o = *ocean surface albedo* = 0.1

σ = *Stefan-Boltzmann constant* = 5.67×10^{-8} .

$L_s = 2.834\times10^6 Jkg^{-1}$ = *latent heat of sublimation for sea ice*

q_{0_s} = *heat of fusion of snow* = $110\times10^6 m^3 J^{-1}$

$C_s = 0.3098\ Wm^{-1}K^{-1}$; $C_i = 2.0344\ Wm^{-1}K^{-1}$ = *thermal conductivity, snow and sea ice*

Appendix B: Heat Flux Computations

For open ocean conditions, H_{To} is the residual of an ocean surface energy balance:

$$H_{To} = R_o - F_o + H_o + E_o \qquad \text{(A1)}$$

where R_o, F_o , E_o and H_o represent net shortwave flux, longwave flux and atmospheric latent and sensible heat fluxes, repsectively, computed using standard formulae. Note that in this computation atmospheric temperature and mixing ratio, T_a and q_a , are utilized as is the ocean temperature T_o, T_a and q_a are defined from the atmospheric model while T_o is calculated by the MLM.

If no snow cover is present on the sea ice, H_{Ti} is calculated similarly to H_{To} except that the incoming total radiation R_i includes the effect of penetration of solar radiation within sea ice, given by the following relation:

$$R_i = (1-i_0)\times(1-\alpha_i)R_s + R_l + i_0\times(1-\alpha_i)R_s\times(1-e^{-1.5h})$$

where R_i is the same as the corresponding variable in Equation (A1) except applicable to the sea ice surface. $i_0 = 0.17$ is the fraction of solar radiation penetration, α_i is the sea ice surface albedo, and h is the thickness of sea ice.

If snow cover is present on the top of sea ice, both sea ice melt and snow melt need to be considered as follows:

$$\left(\frac{\partial h_s}{\partial t}\right)_{therm} = \frac{1}{q_{0_s}}(G_s - H_{T_s}) \qquad \left(\frac{\partial h}{\partial t}\right)_{therm} = \frac{1}{q_0}(H_w - G_i) \qquad \text{(A3)}$$

where h_s = *thickness of snow;*

q_{0_s} = *heat of fusion of snow,*

H_{T_s} = *net energy flux at the snow surface,*

G_s , G_i = *conductive heat fluxes within snow and sea ice, respectively, computed from standard formulae.*

Note that in the computation for G_s and G_i, three temperatures are used: the snow surface temperature, T_s , the sea ice top temperature T_i , and the sea ice bottom temperature T_b (defined as the freezing point of seawater) respectively.

Net energy flux over the snow surface H_{T_s} is computed via a similar energy balance relation as Equation (A1):

$$H_{T_s} = R_{sn} - F_s + H_s + E_s \qquad \text{(A5)}$$

where R_{sn}, F_s, H_s, E_s are the same as the corresponding variables in Equation (A1) except that apply to the snow surface.